A STUDY OF NEOGENE SEDIMENTARY OUTCROPS OF THE GREATER MIRI AREA - CAN CLAY GOUGING BE CALIBRATED IN OUTCROPS AND SHALLOW SUBSURFACE BOREHOLES?

Franz L. Kessler[1,*] and John Jong[2]
[1] *Goldbach Geoconsultants O&G and Lithium Exploration, Germany*
[2] *JX Nippon Oil and Gas Exploration (Deepwater Sabah) Limited*

* *Corresponding Author: franzlkessler32@gmail.com*

ABSTRACT

The greater Miri area offers particularly well-exposed world-class examples of fault geometry and clay gouging. Such information offers good material for studying fault architecture and clay smear morphology, and help to understand fault seal mechanisms in the subsurface. Recent studies on fault and clay gouging in the Neogene sedimentary rocks of greater Miri area show a variety of fault geometries of both abrasive-type and shear-type. In a Nippon Oil-sponsored study carried out in Curtin University, fifteen (15) core holes were drilled through clay-gouged fault planes at three outcrop locations. Cores of the formation were taken, and the drilled holes were then pressurized by water injection for packer testing. The performed leak-off test results were somewhat surprising - weathered Neogene sediments of the Miri and Tukau formations offered little or no pressure retention in fault zones and host rock alike, and leak-off fracturing occurs already at 1.25 bar. The rock mechanics of weathered rock might be very different from fresh rock, and may offer little or no insight into those of virgin rocks. Therefore, weathered rock properties may not be suitable for subsurface fault seal simulation studies.

Keywords: *coring, clay gouging, faults, leak-off, Neogene, sealing, weathering*

INTRODUCTION

Figure 1 shows the regional structural elements of NW Sarawak. The greater Miri area is characterised by moderately folded siliciclastics of Neogene age: the Late Miocene Miri and Lambir formations, and the Pliocene Tukau Formation, as illustrated in Figure 2. The latter forms the subject of the majority of clay gouging studies and pressure testing discussed in this paper. In a recent study, outcrops of the Tukau and Lambir formations were investigated by Curtin University Malaysia (2017). A simplified litho-stratigraphy scheme of the study area is shown in Figure 3 (Jong and Kessler, 2017a):

- The Tukau Formation unconformably overlies the Lambir/Miri formations and is formed by intertidal clastics, in particular tidal channel deposits, which appear strongly amalgamated, and are interbedded with silty parallel layers. Individual channel beds are often characterised by 'side-stepping' and asymptotic foresets, in which laminae can consist of thin, gray claystone or of lignite (Kessler and Jong, 2015 & 2016).
- The Mid-Late Miocene Lambir and Miri formations form the crestal area of the Bukit Lambir and Miri Hills (Figure 2). These formations contain about equal amounts of claystone and sandstone, the latter mainly formed by (sometimes nested) tidal channels and beach bars. Most channels are 'reworked' and strongly amalgamated (Kessler and Jong, 2015 & 2016)
- Clay gouging is seen both in the Pliocene Tukau beds, and the slightly older (Late Miocene) Lambir and Miri formations

This paper summarizes work carried out in Curtin University of Malaysia, Miri. Data were acquired from 2009 to 2013 by the authors, and a later complimentary study was carried out by Curtin students. Furthermore, Geo-Services Kuching performed a shallow drilling campaign on a Nippon Oil-sponsored study, in which a total of fifteen (15) sedimentary cores were taken at three outcrop locations from the Lopeng, Tanjung and Bekenu sites (Figure 4 and Table 1).

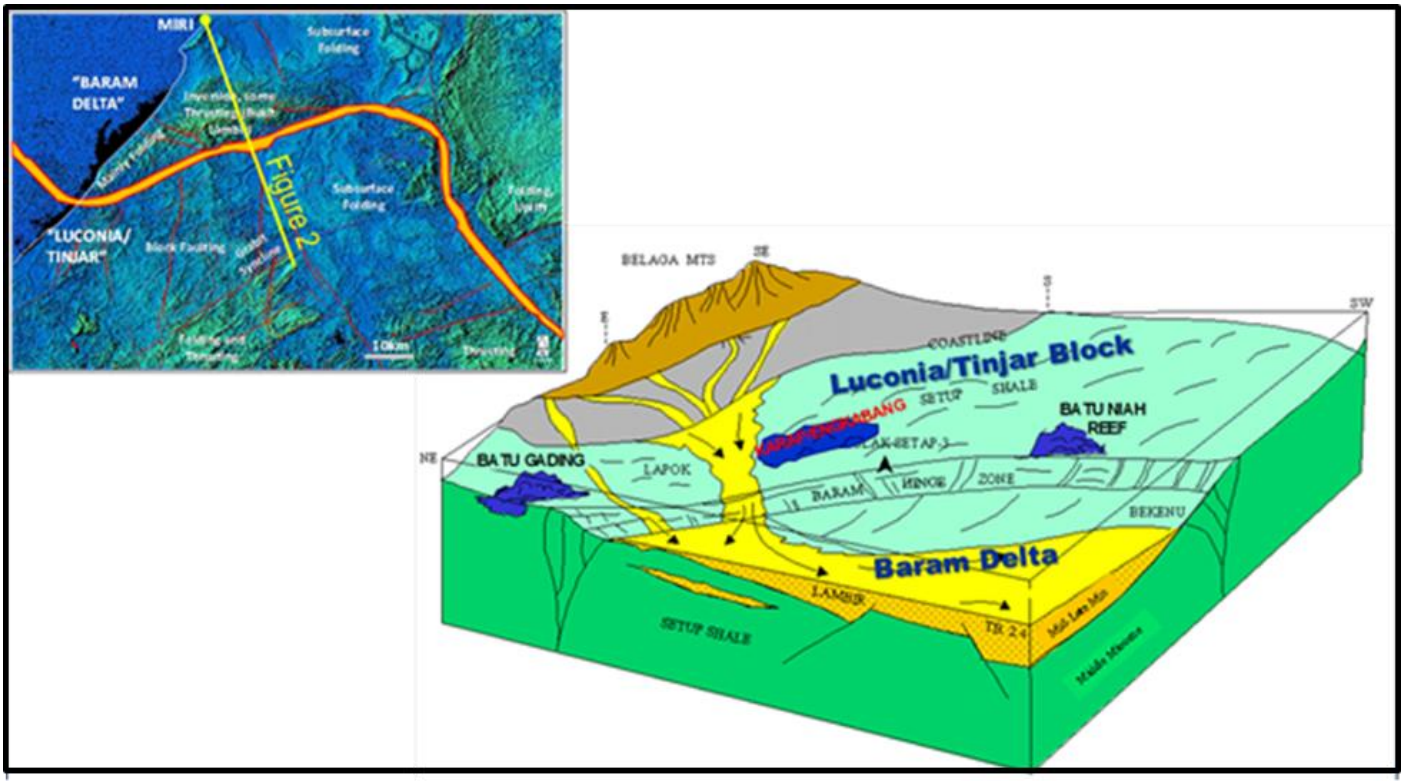


Figure 1: *Schematic block diagram of NW Sarawak with a regional perspective of Late Miocene/Pliocene times. Luconia/Tinjar Block constitutes the footwall, the Baram Delta the hanging-wall NW of the Baram Hinge Zone. The orange Baram/West Baram Line shown in the inset map constitutes an important facies boundary, with carbonates prevailing in Luconia/Tinjar and clastics in the Baram Delta Block. Given the folding of areas such as the Belait-Badas Syncline, Bukit Lambir, Miri etc., NW Sarawak serves as an example of relief-inversion (from Kessler, 2010; Jong et al., 2016).*

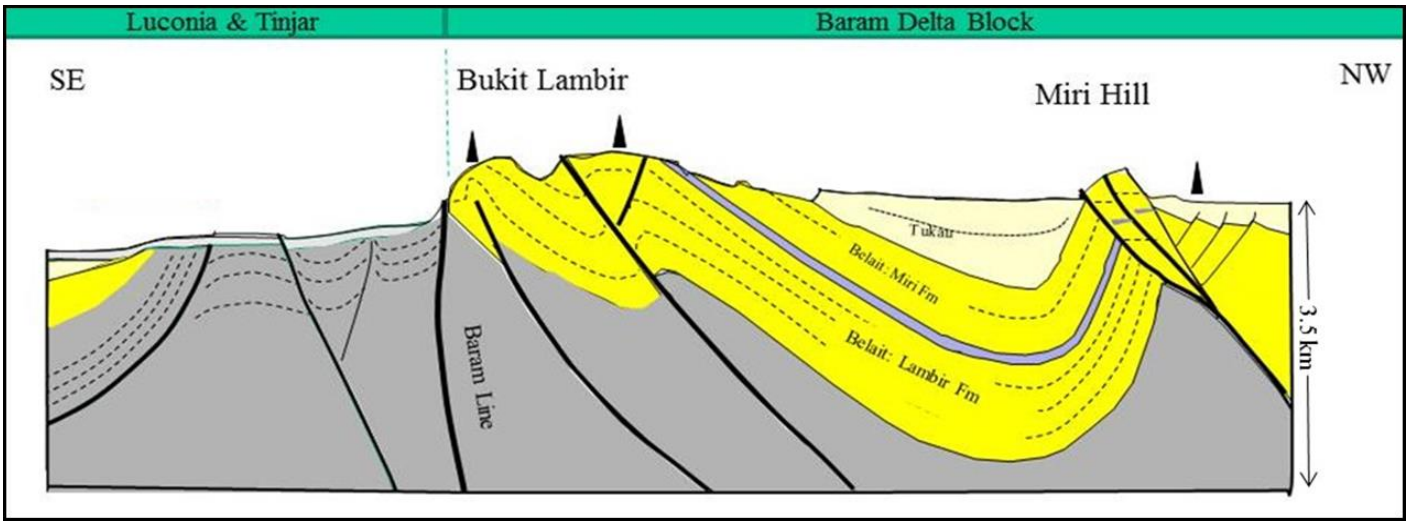


Figure 2: *Tectono-stratigraphic cross-section showing folded Neogene sediments. See Figure 1 inset map for line location. The black triangles indicate the approximate positions of old exploration wells. From Kessler and Jong (2016).*

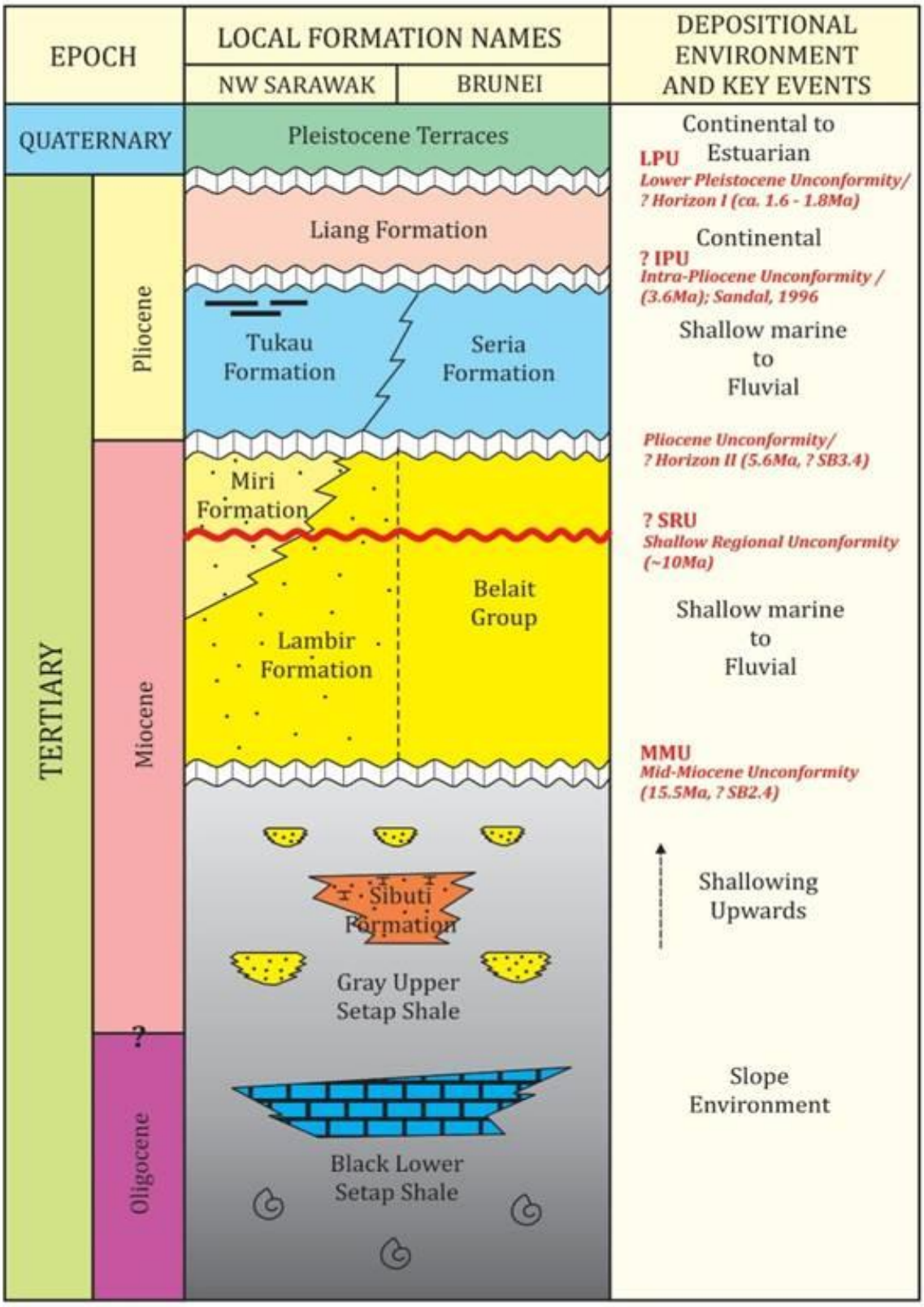


Figure 3: *Simplified litho-stratigraphy scheme of the study area. The term Miri Formation is generally used in the greater Miri area and is age-equivalent to the upper section of the Lambir Formation, Sandal (1996) however, placed the formation partially age-equivalent to the lower Tukau Formation. Likewise, the mid Early Miocene Sibuti Formation is more locally confined with the Subis Limestone Member deposited in the lower part of the Gray Upper Setap Shale (Banda and Honza, 1997). Carbonates are also widespread in the Palaeogene section, and are seen in a number of outcrops and wells (e.g., Batu Niah, Engkabang-1; Jong et al., 2016). The observed unconformity events as annotated are established by Kessler and Jong (2017a), and modified after Kessler and Jong (2015).*

RECENT CLAY GOUGING STUDIES OF THE GREATER MIRI OUTCROPS

In a study of fault geometry and clay gouging of Miri outcrops by Kessler and Jong (2017b), the authors observed a good correlation between normal fault throw, and gouge thickness. It was recommended that the studied outcrops might offer research potential in the areas of gouge mineralogy, gouge stratification and pressure retention.

In 2017, a group of students under the guidance of A/Professors Dr. Ramasamy Nagarajan and Dr. Prasanna Mohan Viswanathan reviewed some fifty (50) faults in and south of the greater Miri area (Curtin University Malaysia, 2017). These faults are near-surface and are located in the Neogene Lambir and Tukau formations. The following methodology was adopted to measure fault morphology and gouging properties:

- Analyzing the sealing capacity and seal-failure envelope of smeared faults.
- Mapping major faults based on geomorphic evidence using satellite imagery.
- Correlating individual faults to determine the stress regime.
- Determining the significance of stress regime on topography of the study area.

The study area covers an approximate area of 143 km^2. Faults were found at several locations; along Jalan Bakam, Jalan Miri-Bintulu, Jalan Coastal Miri-Bintulu, Tusan Beach and Peliau Beach. They were concentrated at the southwest of the mapped area, specifically along Tusan to Peliau Beach, and along Jalan Bakam (Figure 5).



Figure 4: *Location map of investigated and cored outcrops at Lopeng (BHCU1-6), Tanjung (BHCU7-10) and Bekenu (BHCU11-15) sites of the Tukau Formation in greater Miri area.*

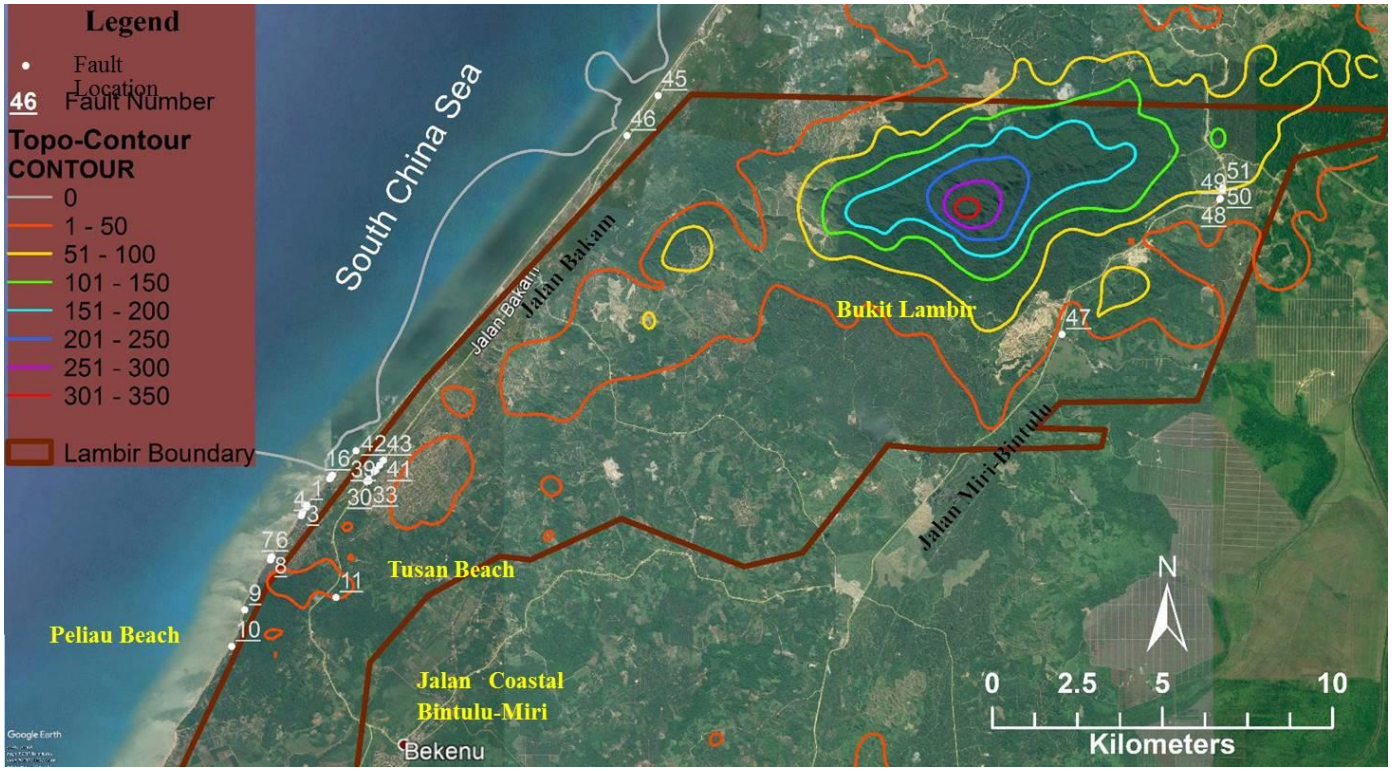


Figure 5: *Basemap of study area with approximate illustration of mapped boundary for Lambir Formation after Liechti et al. (1960) using ArcGIS. The contours as shown are topographic elevations in metres. From Curtin University Malaysia (2017).*

Table 1: *List of diamond drill holes taken in Lopeng, Tanjung and Bekenu outcrop locations in greater Miri area*

Area	Hole No.	Co - ordinates (m)		Surface Elevation (m)	Angle from Horizontal	Bearing Grid	Target Depth (m)
		East	North				
Lopeng	BHCU1	2477805.0	5483714.0	NA	90˚		3.0
	BHCU2	2477823.0	5483612.0	NA	45˚	NE	3.0
	BHCU3	2477815.0	5483630.0	NA	90˚		3.5
	BHCU4	2477807.0	5483648.0	NA	45˚	SE	4.5
	BHCU5	2477818.0	5483660.0	NA	45˚	SE	3.5
	BHCU6	2477815.0	5483658.0	NA	90˚		3.5
Tanjung	BHCU7	2476395.0	5483057.0	NA	45˚	NW	3.5
	BHCU8	2476395.0	5483057.0	NA	45˚	NW	3.5
	BHCU9	2476410.0	5483064.0	NA	45˚	NW	4.5
	BHCU10	2476386.0	5483073.0	NA	45˚	NW	3.5
Bekenu	BHCU11	2460776.0	5456808.0	NA	45˚	NE	3.5
	BHCU12	2460798.0	5456853.0	NA	45˚	NE	3.5
	BHCU13	2460759.0	5456863.0	NA	90˚		3.5
	BHCU14	2460754.0	5456858.0	NA	45˚	NE	3.5
	BHCU15	2460744.0	5456849.0	NA	45˚	NE	6.0

Note: NA = Not Available

Among the faults, smeared faults were reviewed to identify the sealing capacity and seal-failure envelope. They were then broken down into two groups to differentiate between shear- and abrasion-type smears (Figure 6) in order to simplify the calculation on shale gouge ratio (SGR) (Fristad et al., 1997; Yielding, 2002), shale smear factor (SSF) (Lindsay et al., 1992), and clay smear potential (CSP) (Bouvier et al., 1989). The faults were also grouped into relatively recent and older ones to determine the presence of two different stress regimes. Unobserved faults were shown to exist within the region with the aid of software, generating a *Digital Elevation Model (DEM)* using *Global Mapper*, and the application of *Open Topography* and *Google Maps*. The regional fault

strike identified was then compared with the direction of stress regimes determined using stereographic projections obtained from the two age groups of investigated faults. The influence of stress regimes on topography of the area was estimated to be significant.

Seal-failure envelope and sealing capacity of faults were calculated using measurements obtained in the field using measuring tape, such as clay layer thickness, clay width within fault, vertical slip, and distance of the clay smeared. It is well-established that SGR algorithm is widely used to identify the seal behavior under static pressure conditions (Fristad et al., 1997; Yielding, 2002).

SGR = shale layer thickness (m)/vertical slip (m) x 100% (1)

The formula above calculates clay/shale gouge ratio on fault plane surfaces and estimates general seal-failure envelope if needed (Yielding et al., 1997). While CSP and SSF were calculated to compare and highlight the consistency and accuracy of sealing capacity calculated using SGR. CSP and SSF were used to calculate for shear-type smears, whereas only SSF is calculated on abrasion-type smears.

CSP = $C\Sigma$ (mud layer thickness)^2 (m^2)/distance of clay smear (m) (2)

With SGR determined, sealing capacity curves can be used as a guide for geologists conducting oil and gas exploration in the region. By mapping major faults based on geomorphic evidence using satellite imagery, faults not observed in the field can be interpreted and it can be determined whether they are associated with the surrounding smeared faults. The stress regime influences the topography of the study area, while the paleo-stress regime can be linked with relatively recent stress regimes to provide a better understanding of the area's terrain and its significance on structural hydrocarbon trapping.

By calculating amount of clay within its surrounding sediment, the probability of smearing of faults can be determined. A calibration constant, C, is added into the formula only when discontinuous shear-type smear is present (Vrolijk et al., 2016; after Bouvier et al., 1989). The calibration constant, C, depends on the rheology and competency of a rock at a certain depth. C values were obtained from Bretan et al. (2003) where C = 0.5, 0.25 and 0 at burial depths of shallower than 3 km, 3 to 3.5 km, and deeper than 3.5 km, respectively. The SSF formula determines the likelihood of continuous smearing by measuring the slip of the fault and surrounding mud layer thickness (Lindsay et al., 1992).

SSF = vertical slip (m) / shale layer thickness (m) (3)

Only nineteen (19) of the shear- and abrasion-type faults investigated were found to be smeared in the area (Table 2). Abrasion-type faults have no value for distance of clay sheared and hence calculation of CSP is impossible. Based on Table 2, a cross-plot of SSF and SGR is generated to illustrate the seal-failure envelope for the smeared faults in the area with respect to continuity of clay smears (Figure 7). As stated by Lindsay et al. (1992), faults with SSF greater than 7 are considered as faults with discontinuous smears or faults with failed seals. Hence, the seal-failure envelope was determined by plotting SSF equals 7 to find the corresponding SGR value.

In the Lambir Formation the boundary between non-sealing and sealing faults for SGR value was expected to be approximately 15% to 20%, similar to that in the Niger Delta (Fristad et al., 1997; Yielding, 2002), albeit comparatively lower than those estimated for the West Baram Delta fields with an overall SGR threshold of > 20% for effective trapping. From the cross-plot (Figure 7), an inverse relationship between the two algorithms, where SGR increases with decreasing SSF can be seen. The SGR found for the seal-failure envelope is 14%, which is quite close to that from Niger Delta, and hence faults with SGR of 14% and below is expected to have discontinuous smears, resulting in non-sealing faults.

As Bouvier et al. (1989) and Jev et al. (1993) agreed that CSP data are more qualitative than SSF and SGR, a cross-plot was plotted with respect to CSP and SGR (Figure 8). It is noted that no trend, pattern or relationship between the data can be determined. This could be due to the fact that a lack of data for shear-type smears prevents the construction of a decent cross-plot similar to that generated by Oyedele and Adeyemi (2009). However, from Table 3, CSP with values greater than 30 reflects SSF less than 7. By combining both theories from Lindsay et al. (1992) and Jev et al. (1993), faults with CSP greater than 30 are believed to generate continuous smear along fault lines.

For the estimation across fault pressure differences (AFPD; Bertan et al., 2003), fault data with SSF values less than 7 were disregarded, together with those of CSP values less than 15, since these values suggest discontinuous smears and are less likely to generate smear forming seals. Graphs of AFPD and hydrocarbon column height (HCH) versus SGR, CSP and SSF assuming a light oil were also constructed with HCH calculated using calibrated fault-seal attributes (Figure 9). From the graphs, the minimum and maximum amounts of pressure sustainable for the smeared faults in the

Lambir Formation at depths less of than 3 km are 0.32 and 0.46 bar, respectively (Table 4). The estimated range of HCH of light oil that can be maintained in those depths and pressures is 13.24 to 18.84 m (Table 4).

In summary, the study found that Lambir Formation has seal-failure envelope at SGR of 14%, even though siliciclastic sequences were determined to have common seal-failure envelopes for SGR ranging from 15% to 20%, or higher. Overall, there is no sound correlation between fault throw and clay gouging thickness. Regional fault strike and identified stress regimes were determined to be both parallel and perpendicular to each other. The Lambir Formation was found to be dominated by normal faults, with some reverse and strike-slip faults. However, in an earlier study, Kessler and Jong (2017b) provided data which suggest that such a correlation might exist (Figure 10). Nonetheless, this and other studies suffer from the fact that small faults are more common and large faults are more rarely found in outcrops. In a nutshell, although outcrop studies as carried out here can provide insight into important processes that shape traps and retention parameters alike, it is not clear whether such measurements can be applied for simulation of subsurface fault seal retention – the jury is still out.

CORING AND PRESSURE TESTING OF FAULTED NEOGENE SEDIMENTARY ROCKS

Fieldwork and core drilling were carried out from 10th to 22nd June, 2010 at three outcrop locations from the Lopeng, Tanjung and Bekenu sites (Figure 4 and Table 1). Activities were as follows:

- The preparatory work consisted of a detailed mapping of the areas surrounding faulted sequences; this was carried out in distinct phases - Work by Kessler and Jong (2010) and Kessler et al. (2010), as well as mapping conducted by Curtin University Malaysia's student final semester study projects for the degree of Bachelor of Science in Applied Geology. Estimations of fault cut and measurements of gouging material, thickness were carried out. Taking account of critical parameters such as road access and availability of water supply, the three study locations were selected.

- The contractor Geo-Services mobilized drilling rig and packer testing equipment from Kuching and drilled shallow core holes (less than 8 m) through the previously flagged faulted and clay-gouged sequences. The cores were pulled, described and packed and sent to Curtin University Malaysia for further analysis.

- Packers were set above and below the faulted and gouged zone. The contractor injected water, pressured up the formation and monitored the flow rates and pressures. In such way the leak-off pressures could be established.

- Procedures and results were documented in a report.

Figure 11 shows the outcrop views of the three locations.

FIELD INVESTIGATION METHOD

One unit of a hydraulic drilling machine *YBM – YS01* was used to carried out the rotary boring and rock coring tasks. Advancement of the open holes were achieved by loosening the soil using a roller – bit, drag bit, and flushing out the loose material by means of circulating water under high pressure. Casings were used to stabilise the open holes. *NMLC* triple tube core barrels were used for coring the hard formation such as sandstone and mudstone. Cores are removed from the triple tube core barrel by the application of steady hydraulic pressure to the inner tube. Immediately upon extraction, the cores are placed in the order of extraction in the core box with increasing depth from left to right within each partition, and with increasing depth from top to bottom, when the observer faces the box from the unhinged long edge. Details of the rock type, depth, weathering degree, details of mineralisation, orientation of fractures and joints are recorded in borehole logs (Table 5). Shifting of the drilling machines within the site was supported by the *Yanmar* steel track crawler carrier, and the *Toyota Carrier.*

Fifteen (15) diamond drill holes, namely BHCU1, BHCU2, BHCU3, BHCU4, BHCU5, BHCU6, BHCU7, BHCU8, BHCU9, BHCU10, BHCU11, BHCU12, BHCU13, BHCU14, and BHCU15 were drilled with six (6) boreholes at Lopeng area, four (4) boreholes at Tanjung area, and five (5) boreholes at Bekenu site along Jalan Coastal Miri-Bintulu (Figure 4 and Table 1). A total of 56 m of sedimentary rocks were cored from the three mentioned areas. For all diamond drill holes, detailed logs and drill core photographs are kept and recorded (Table 5).

All diamond drill holes were water pressure tested during the course of drilling. Water pressure tests (packer test) were carried out on all holes after every 1.5 m to 2.0 m of rocks had been cored as drilling progressed. A single *Packer Bimber 11* was used with a high pressure Nitrogen cylinder to inflate the packer at 11 bars. A total of thirty-six (36) water pressure tests were carried out at the sites (Table 6). Ground water levels were recorded on a regular basis, the readings being taken before

and after drilling. The date and time of readings, borehole depth, and length of casing below the ground at the time of reading were also recorded in the borehole log (e.g., Table 5).

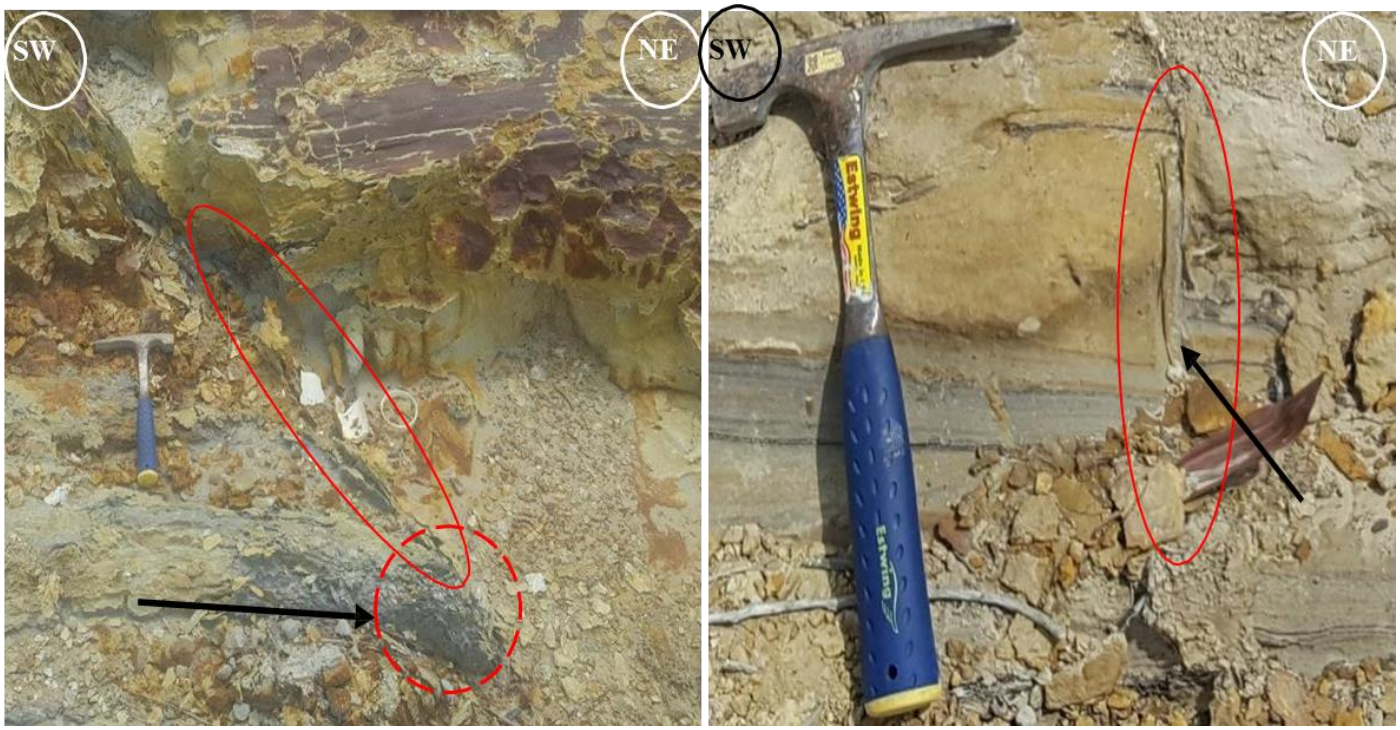


Figure 6: *Field image taken as an example for shear-type smear (left, Fault 40) and abrasion-type smear (right, Fault 19). The hammer is placed as scale with length of 28 cm. The red oval areas are examples of shear smear and deformed rock shown in red dashed circle (from Curtin University Malaysia, 2017).*

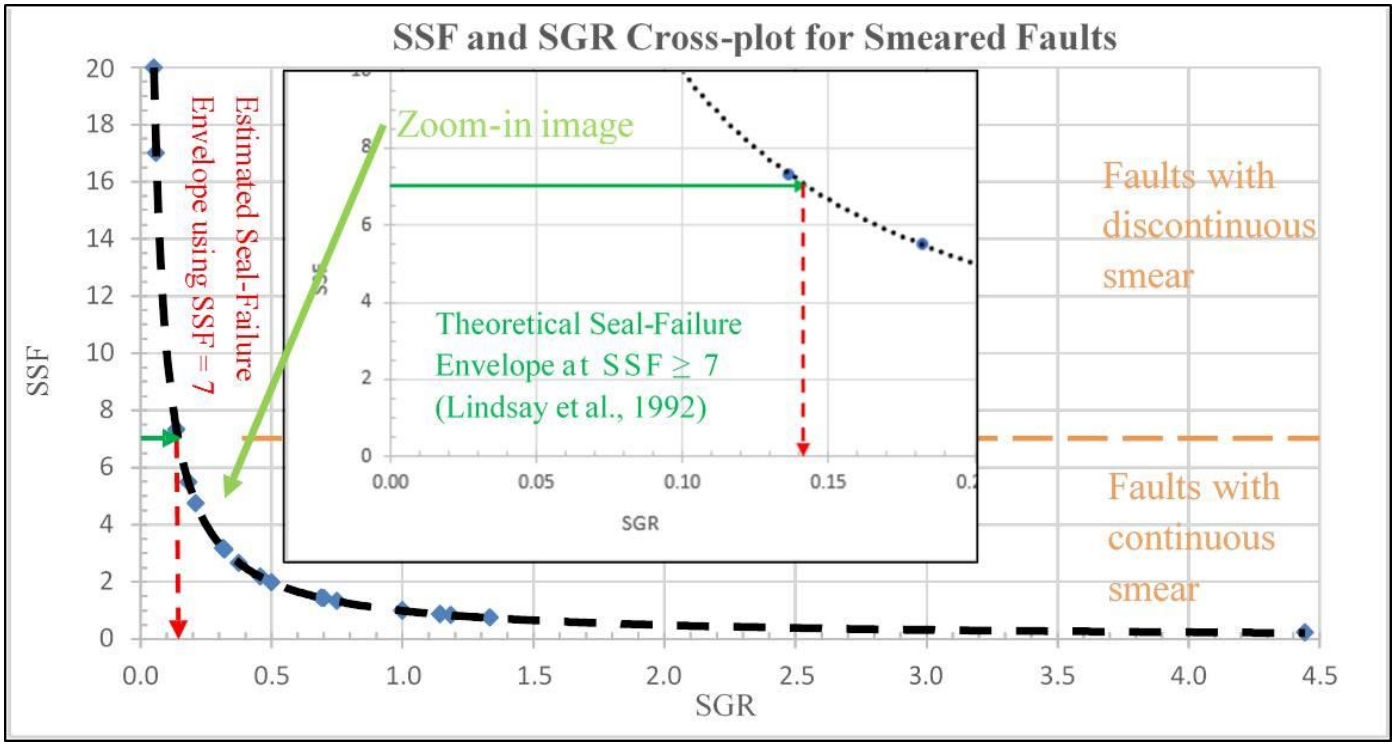


Figure 7: *Cross-plot of SSF (shale smear factor) and SGR (shale gouge ratio). for smeared faults in the study area to determine seal-failure envelope (from Curtin University Malaysia, 2017 and after Oyedele and Adeyemi, 2009). The plot serves as a model for smeared faults found near and within the region to determine the continuity of smears based on calculated SSF and SGR.*

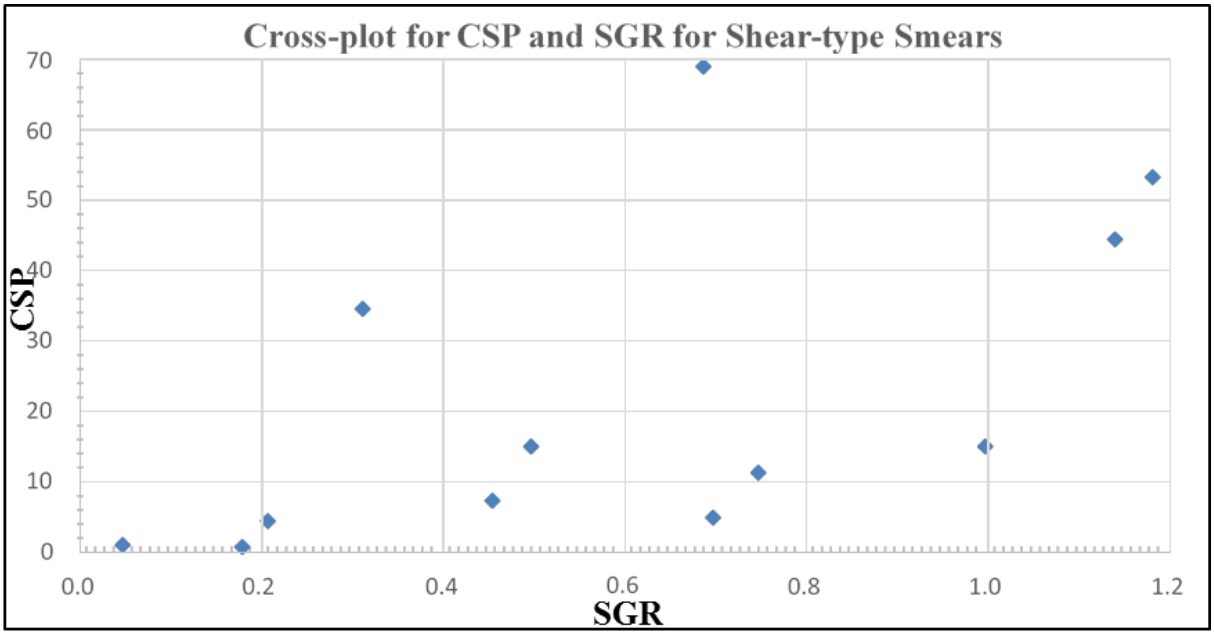


Figure 8: *Cross-plot of CSP (clay smear potential) and SGR (shale gouge ratio) for smeared faults in the study area (from Curtin University Malaysia, 2017 and after Oyedele and Adeyemi, 2009).*

Table 2: *Statistical data for calculation of SGR, SSF and CSP for smeared faults. It is found that abrasion-type smears in the area have clay smear width of less than 5 cm, while shear-type smears can range from centimetre to metre scale. Abrasion smears were identified easily whereby smears along the fault lines seems to be distorted due to the shear stress generated from faulting (from Curtin University Malaysia, 2017). See Figure 5 for location map of investigated faults.*

Fault	Mud/Clay Layer Thickness (cm)	Clay Smear Width (cm)	Vertical Slip (cm)	Distance of Clay Sheared (cm)	SGR (Eq. 1)	CSP (Eq. 2)	SSF (Eq. 3)
2	20.00	3.00	4.50	Abrasion-type fault	4.44	-	0.23
7	40.00	1.00	35.00	18.00	1.14	44.44	0.88
8	15.00	2.00	15.00	15.00	1.00	15.00	1.00
17	7.00	0.50	10.00	10.00	0.70	4.90	1.43
19	12.00	1.00	9.00	Abrasion-type fault	1.33	-	0.75
21	4.00	7.00	22.00	22.00	0.18	0.73	5.50
22	3.00	1.00	22.00	Abrasion-type fault	0.14	-	7.33
23	1.00	0.50	17.00	Abrasion-type fault	0.06	-	17.00
25	20.00	2.50	400.00	400.00	0.05	1.00	20.00
27	3.00	3.00	8.00	Abrasion-type fault	0.38	-	2.67
31	100.00	3.00	145.00	145.00	0.69	68.97	1.45
34	30.00	8.00	60.00	60.00	0.50	15.00	2.00
35	21.00	5.00	100.00	50.00	0.21	4.41	4.76
36	16.00	2.00	35.00	35.00	0.46	7.31	2.19
37	15.00	3.00	20.00	20.00	0.75	11.25	1.33
40	45.00	9.00	38.00	38.00	1.18	53.29	0.84
44	8.00	4.00	25.00	Abrasion-type fault	0.32	-	3.13
46	110.00	100.00	350.00	350.00	0.31	34.57	3.18
48	45.00	3.50	45.00	Abrasion-type fault	1.00	-	1.00

Table 3: *Data for shear-type smear faults with respect to increasing CSP value; green values indicate potential sealing faults modelling by Curtin University Malaysia (2017). See Figure 5 for location map of faults*

Fault	Shale/Clay Layer Thickness (cm)	Clay Smear Width (cm)	Vertical Slip (cm)	Distance of Clay Sheared (cm)	SGR (Eq. 1)	CSP (Eq. 2)	SSF (Eq. 3)
21	4.00	7.00	22.00	22.00	0.18	0.73	5.50
25	20.00	2.50	400.00	400.00	0.05	1.00	20.00
35	21.00	5.00	100.00	50.00	0.21	4.41	4.76
17	7.00	0.50	10.00	10.00	0.70	4.90	1.43
36	16.00	2.00	35.00	35.00	0.46	7.31	2.19
37	15.00	3.00	20.00	20.00	0.75	11.25	1.33
8	15.00	2.00	15.00	15.00	1.00	15.00	1.00
34	30.00	8.00	60.00	60.00	0.50	15.00	2.00
46	110.00	100.00	350.00	350.00	0.31	34.57	3.18
7	40.00	1.00	35.00	18.00	1.14	44.44	0.88
40	45.00	9.00	38.00	38.00	1.18	53.29	0.84
31	100.00	3.00	145.00	145.00	0.69	68.97	1.45

Table 4: *Statistical data for light oil AFPD and HCH calculation with order of increasing SGR (from Curtin University Malaysia, 2017). C = calibration constant, AFPD = across fault pressure difference, HCH = estimated hydrocarbon column height.*

Fault	Sealing Capacity			C = 0.5 (< 3 km)		C = 0.25 (3 to 3.5 km)		C = 0 (> 3.5 km)	
	SGR	CSP	SSF	AFPD (bar)	HCH (m)	AFPD (bar)	HCH (m)	AFPD (bar)	HCH (m)
46	0.31	34.57	3.18	0.32	13.24	0.58	23.55	1.03	41.88
44	0.32	-	3.13	0.32	13.25	0.58	23.56	1.03	41.90
27	0.38	-	2.67	0.33	13.31	0.58	23.67	1.03	42.10
34	0.50	15.00	2.00	0.33	13.46	0.59	23.93	1.04	42.55
31	0.69	68.97	1.45	0.34	13.68	0.60	24.32	1.06	43.24
8	1.00	15.00	1.00	0.34	14.04	0.61	24.97	1.09	44.40
48	1.00	-	1.00	0.34	14.04	0.61	24.97	1.09	44.40
7	1.14	44.44	0.88	0.35	14.21	0.62	25.28	1.10	44.95
40	1.18	53.29	0.84	0.35	14.26	0.62	25.37	1.11	45.11
19	1.33	-	0.75	0.35	14.45	0.63	25.69	1.12	45.69
2	4.44	-	0.23	0.46	18.84	0.82	33.50	1.46	59.57

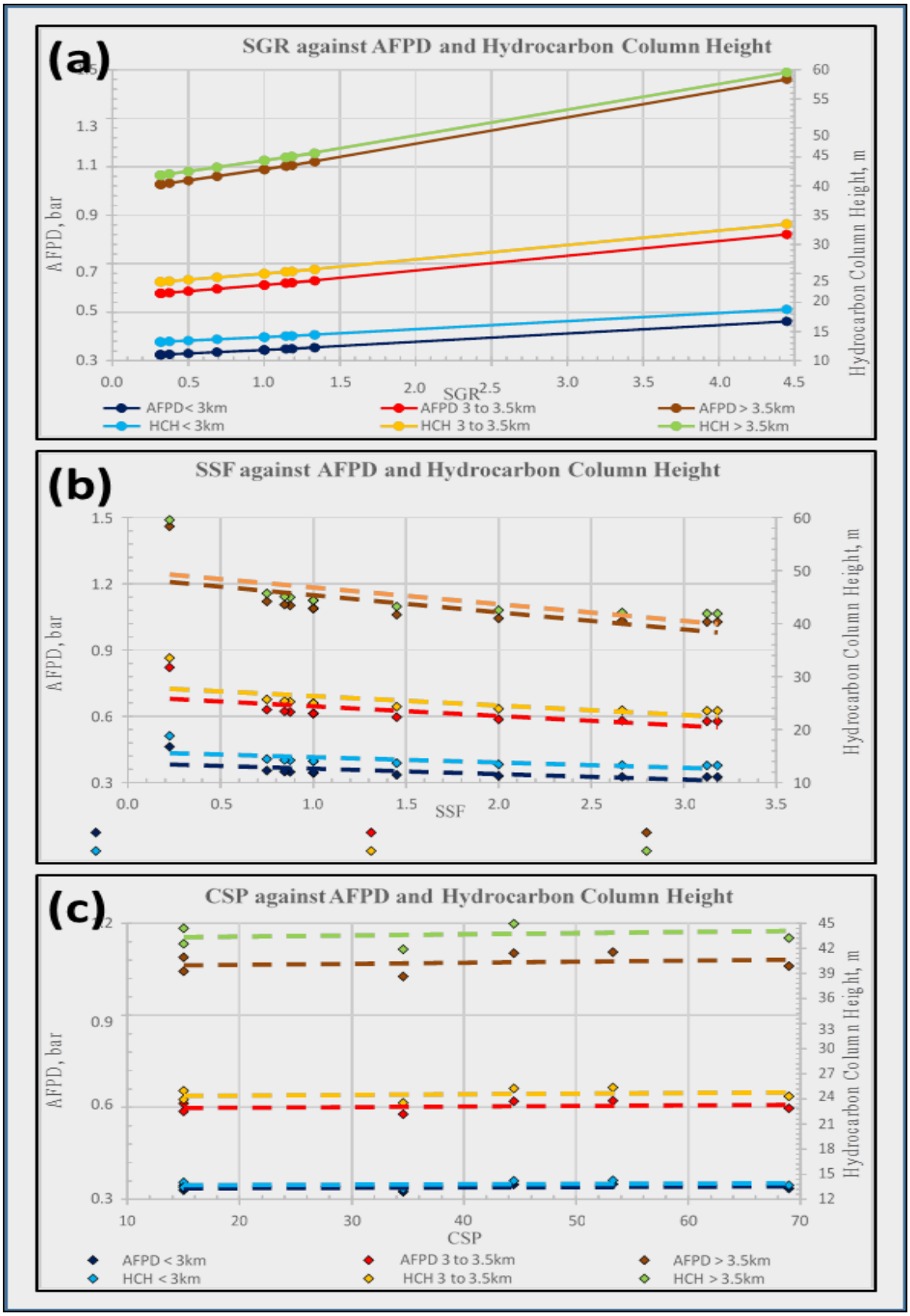


Figure 9: *Graphs of (a) SGR (b) SSF, and (c) CSP against AFPD and HCH in different depth intervals (from Curtin University Malaysia, 2017 and after Bretan et al., 2003). SGR = shale gouge ratio, SSF = shale smear factor, CSP = clay smear potential, AFPD = across fault pressure differences, HCH = hydrocarbon column height.*

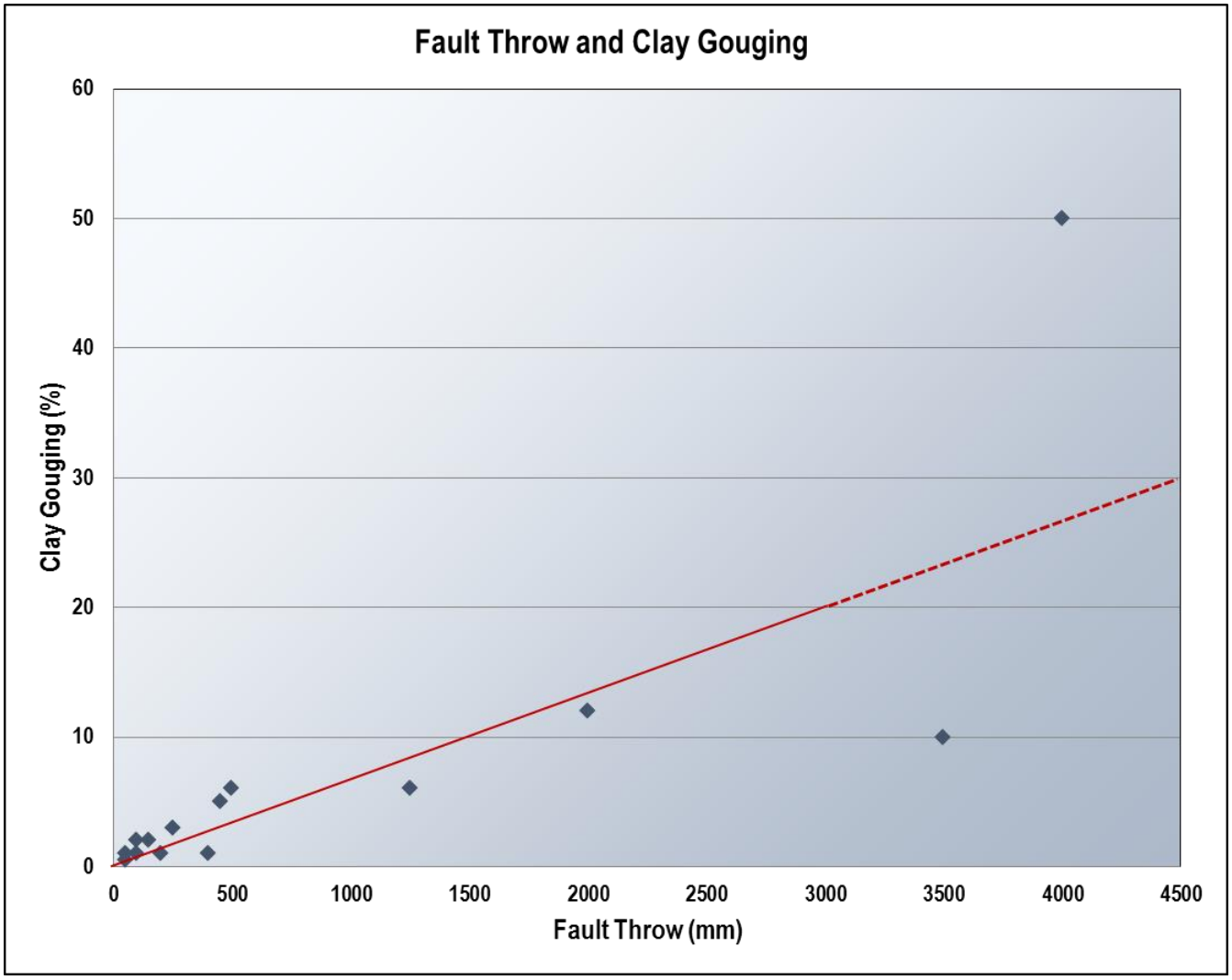


Figure 10: *Small fault throws result in thin layers of clay gouging, whereas large fault throws offer thicker layers of clay smear. Note the lack of data points for fault throws of more than 2000 mm resulted in an unreliable trend line for throw values of more than 3000 mm. However, this trend may be substantiated with more data, and may be useful to predict potential hydrocarbon columns in fault-traps. From Kessler and Jong (2017b) and data from Kessler and Jong (2010).*

RESULTS, DISCUSSION AND CONCLUSIONS

Estimation of SGR - A Reliable Input Parameter?

The greater Miri area offers many particularly well exposed fault outcrops and forms an ideal location to make use of cores to test the gouged fault zones for pressure retention. The ultimate goal remains to estimate gouging material thickness in relation to fault throw, and forecast column height of hydrocarbons that can be trapped in fault-closed trap compartments (e.g., Kessler and Jong, 2017b; Curtin University Malaysia, 2017). Unlike the mentioned outcrop study conducted by Curtin University Malaysia (2017), the estimated pre-drill subsurface SGR threshold for trapping in the Adong Kecil West oil and gas discovery (located along the proven Miri-Rasau anticline) was simulated using the software *Faultseal™,* and was found to be significantly higher, requiring an SGR in the order > 20% for effective trapping of hydrocarbons and comparable with the data from the West Baram Delta fields (Jong and Shimada, 2009).

In a recent case study of the same discovery by Uchimura et al. (2014), it was noted that the trapping fault has the largest throw in its central part and dies out laterally and downward. However, 350m of net hydrocarbon column in six (6) sandstone horizons was discovered trapped by the lower part of the fault, where its throw was minimal (Figure 12). Since the fault throw is smaller than the sandstone thickness, extensive sand-to-sand juxtaposition can be expected unless there is a continuous clay smear. New 3D seismic data acquired after the discovery was interpreted in detail around the fault block and careful editing was made to depth converted maps to establish the detailed fault framework model. Firstly, juxtaposition across the fault was identified based on the 3D model. Secondly, quantitative fault sealing capacity analyses for SGR and SSF were performed along individual fault planes using fault throw and Vsh at each cell using *Structural and Fault Analysis (RDR)* module in *Petrel.* Thirdly, the SGR model was converted to a maximum potential HCH.

Despite the fact that the fault throw is much smaller than the thickness of the entire sand body, SGR in some areas of sand-to-sand juxtaposition still showed more than 20%, which is generally considered to be the minimum number for continuous clay smear over such an interval. This is due to a contribution of shaliness from the sandstone that contains thin, but frequent intercalations of minor clay/silt. However, potential HCHs calculated from SGR were only up to 20 m, while the observed hydrocarbon column in the well reached more than 80 m. The regional characteristic clay extension indicated that the chance of having good seal in the interval was quite low.

To explain the abnormally trapped hydrocarbon, the authors suggested that the sealing capacity of faults could have been reinforced with additional lateral and/or vertical clay injection into the fault plane. Lateral clay injection into normal faults in the greater Miri area based on outcrop observation and model experiments has been described by van der Zee et al. (2003) and van der Zee and Urai (2005). This may be one of the effective mechanisms for trapping potentially longer hydrocarbon columns in the West Baram Delta. Considering that hydrocarbons were found only associated with the deeper part of the fault, vertical clay injection from the underlying mobile Setap Shale could be another important mechanism. Pro-delta shale is widely distributed in the West Baram Delta as muddy distal facies and is widely known to be over-pressured with mud diapirs and clay ridges both well-known in the study area (Kessler and Jong, 2014).

The many uncertainties in respect to the lateral extent of fault seals and gouging thickness suggest that one should try to compare simulated results with empirical findings from proven hydrocarbon systems. Figure 13 illustrates the fact that clay smear and gouging may be only one of the many factors that define a fault-bounded hydrocarbon trap. It is noted that as dictated by the sandier nature of deltaic sediments, small hydrocarbon accumulations are more common in the nearby offshore West Baram Delta and offshore Brunei shelf with stacked oil and gas reservoir pays resulting from small fault throws, while long hydrocarbon columns appear to be rare. Such empirical data can be very useful in Montecarlo simulations. The P_{50} value may be in the order of 15 m, and hydrocarbon column length significantly beyond 100 m may be a smaller than P_5 probability only.

Pressure Testing in Shallow Outcrop Boreholes

The pressure testing results, however, yielded valid yet surprising conclusions:

- Leak-off tests showed, that neither sandy rocks nor gouged zones offer any significant plumbing, and that the pressure-tested rock fractures or faults failed at *ca.* 1.25 bar or 18.13 psi irrespective of the material tested; which in conclusion, suggests that the rock behaved extremely softly.



Figure 11: *View of Tukau Formation outcrops at Lopeng, Tanjung and Bekenu coring sites.*

Table 5: *An example of a core boring report taken from BHCU15 location with interpreted borehole log.*

Geo-Services

CORE BORING REPORT — **BORING NO.** BHCU15

PROJECT: Rock Coring & Packer Test in the Fault Zone Of The Miri Formation.
CLIENT: CURTIN UNIVERSITY, MIRI
CONTRACTOR: Geo-Services
EQUIPMENT USED: YBM 2 with Crawler mounted

JOB NO:
PAGE NO: 1 of 1
ELEVATION:
DATE START: 22-06-10
DATE FINISH: 23-06-10
DRILLER: Alias/Wan
PREPARED BY: Richard
LOCATION: Bekenu Coastal Road, Miri ,Site

GROUND WATER			DEPTH TO:				ORIENTATION	CORE BARREL	
DATE	Time	HRS A/FT	WATER	CASING	HOLE depth		VERTICAL	TYPE:	NMLC
22-06-10	1515hrs	AD	1.10 mbgl	0.5m	1.5m		HORIZONTAL	SIZE:	76mm
22-06-10	1505hrs	AD	1.26 mbgl	1.5m	3.0m	45°	INCLINED	Bit(mm)	150mm
22-06-10	1800hrs	AD	2.30 mbgl	1.5m	450m		BEARING	Barrel(mm)	1372mm
23-06-10	1050hrs	AD	3.54 mbgl	1.5m	6.00m		ANG FROM VERT.	Total(M)	1.52M

Elevation (m)	DEPTH IN m	Casing Depth m	CORE run DEPTH RANGE	Core run	Core Run No.	Packer T	Core Data Run m	Core Data Recov %	Core Data RQD %	GRAPHIC LOG	FIELD CLASSIFICATION AND REMARKS
	0.5	0.5									**-Silty Sandstone/Shale**, Yellowish Grey, Mod. - Highly weathered,
	1		0.0-1.5	C1			1.5	73	18		interbedded with Shale and Siltstone, Dipping 60°-75° easterly.
	1.5	1.5									**-Silty Sandstone**, Grey, Weak, Mod. - Highly weathered, Planar,
	2										Fine Grained, Latd shale, V Close joints filled w/ argillaceous material.
	2.5		1.5-3.0	C2			1.5	47	81		**-Silty Sandstone** Grey, Weak, Moderate - Highly weathered,
	3										parting, Interlamination w/ Shale .Joints
	3.5										Fault plane at 1.9m . B.g.l. Planar, Joints 60°-80°filled w/ argillaceous
	4		3.0-4.5	C3			1.5	57	63		**-Silty Sandstone**, Grey, Weak, Mod. - Highly weathered, Planar,
	4.5										Fine Grained, Latd shale, V Close joints filled w/ argillaceous material.
	5										
	5.5		4.5-6.0	C4			1.5	45	91		**-Silty Sandstone**, Grey, Weak, Mod. - Highly weathered, Planar,
	6										Fine Grained, Latd shale, V Close joints filled w/ argillaceous material.
	6.5										
	7										Coring in borehole terminated at 6.0 m b.g.l., and four numbers of
	7.5										Packer tests were performed . at interval 0.5m - 1.5m and
	8										1.5m - 3.05m, 3.0m - 4.5m, and 4.5m - 6.0m respectively.
	8.5										
	9										***Packer Test No. PKTBHCU15-1 (0.5m - 1.5m)***
	9.5										
	10										***Packer Test No. PKTBHCU15- 2(1.5m - 3.0m)***
	10.5										
	11										***Packer Test No. PKTBHCU15- 3(3.0m - 4.5m)***
	11.5										
	12										***Packer Test No. PKTBHCU15- 4(4.5m - 6.0m)***
	12.5										
	13										Datas of packer tests refer to packer test sheets.
	13.5										
	14										
	14.5										

FIELD HARDNESS		BEDDING		ATTITUDE AND ANGLE	JOINTS/SHEAR/FRACTURE		WEATHERING
V. HARD	-KNIFE CAN SCRATCH	V. THIN	<2"	HORIZONTAL (0 - 5°)	V. CLOSE	<2"	FRESH
HARD	-SCRATCHES DIFFICULT	THIN	2" - 12"	SHALLOW OR LOW ANGLE (5 - 35°)	CLOSE	2" - 12"	V. SLIGHT
MOD HARD	-SCRATCHES EASILY	MEDIUM	12" - 36"	MODERATELY DIPPING (35 - 55°)	MOD. CLOSE	12" - 36"	SLIGHT
SOFT	-GROVES	THICK	36" - 120"	STEEP OR HIGH ANGLE (55 - 85°)	WIDE	36" - 120"	MODERATE
V. SOFT	-CARVES	V. THICK	>120"	VERTICAL (85 - 90°)	V. WIDE	>120"	MOD. SEVERE
							COMPLETE

Table 6: *Examples of leak-off testing reports from PKTCU9-1(left) and PKTCU15-1 (right).*

GEO-SERVICES — PACKER OR LUGEON TEST

Packer or Lugeon test sheet		Site: Miri Tanjung site	Location: Miri Tanjung Site	
Depths below ground Level to		Job No:	Borehole No: BHCU9	
a) top of the test section:	0.5 m	Date: 18/06/2010	Sheet: 1 of 1	
b) bottom of test section:	1.5 m	Ground level:	Crew/Operator: Alias/Wan/ Freddie	
c) centre of test section:	0.5-1.5 m	(ordinance datum)		
d) bottom of hole at time of test:	1.5 m	Weather: Raining	Test No: PKTCU9-1	
e) bottom of casing:	0.5 m	Packer pressure: 11bar		
f) initial ground water level:	0.4 m	Packer Type: Single Packer Bimbar 11		
		Dia. Of hole in test area: 76 mm		
Gauge height above ground level:	0.3 m	Type of Rock: Weathered Silty Sandstone		

Test record

1st period	Time, min	**0**	**1**	**2**	**3**	**4**	Average flow
Gauge Pressure:	Flowmeter	18429	18445	18461.1	18476.1	18491.2	q litres/min
	Dipmeter		***Pressure dropped to zero***				
1.25 bar	Water take litre		160	161	150	151	155.5
2nd period	Time, min	**0**	**1**	**2**	**3**	**4**	Average flow
Gauge Pressure:	Flowmeter	18509	18524.2	18538.5	18553.1	18568.1	q litres/min
	Dipmeter		***Pressure dropped to zero***				
0 bar	Water take litre		152	143	146	150	147.75
3rd period	Time, min	**0**	**1**	**2**	**3**	**4**	Average flow
Gauge Pressure:	Flowmeter	18572	18586.8	18596.1	18609.1	18624.2	q litres/min
	Dipmeter		***Pressure dropped to zero***				
0 bar	Water take litre		148	93	130	151	130.5
4th period	Time, min	**0**	**1**	**2**	**3**	**4**	Average flow
Gauge Pressure:	Flowmeter	18629.1	18644.1	18658.9	18673.8	18688.8	q litres/min
	Dipmeter		***Pressure dropped to zero***				
0 bar	Water take litre		150	148	149	150	149.25

Remarks:

Leakage along the fault plane about 1.0m away from the fault line can be seen on surface .
Pressure cant be set for the cycle of of test due to leakage along fault plane.

Packer were tested with zero bar for 16 minutes.

GEO-SERVICES — PACKER OR LUGEON TEST

Packer or Lugeon test sheet		Site: Bekenu, Coastal Rd.	Location: Bekenu, Coastal Rd.	
Depths below ground Level to		Job No:	Borehole No: BHCU15	
a) top of the test section:	0.5 m	Date: 23/06/2010	Sheet: 1 of 1	
b) bottom of test section:	1.5 m	Ground level:	Crew/Operator: Alias/Wan/ Freddie	
c) centre of test section:	0.5-1.5 m	(ordinance datum)		
d) bottom of hole at time of test:	1.5 m	Weather: Fair Sunny day	Test No: PKTCU15-1	
e) bottom of casing:	0.5 m	Packer pressure: 11bar		
f) initial ground water level:	1.10 m	Packer Type: Single Packer Bimbar 11		
		Dia. Of hole in test area: 76 mm		
Gauge height above ground level:	0.3 m	Type of Rock: Weathered Silty Sandstone		

Test record

1st period	Time, min	**0**	**1**	**2**	**3**	**4**	Average flow
Gauge Pressure:	Flowmeter	22929	22944.5	22961.5	22977.6	22994.1	q litres/min
	Dipmeter		***Pressure dropped to 0 bar after 1 minutes***				
1.25 bar	Water take litre		155	170	161	165	162.75
2nd period	Time, min	**0**	**1**	**2**	**3**	**4**	Average flow
Gauge Pressure:	Flowmeter	23022	23036	23051.2	23065.7	23080	q litres/min
	Dipmeter		***Pressure dropped to 0 bar***				
0 bar	Water take litre		140	152	145	143	145
3rd period	Time, min	**0**	**1**	**2**	**3**	**4**	Average flow
Gauge Pressure:	Flowmeter	23084.8	23099.9	23114.1	23128.5	23143.2	q litres/min
	Dipmeter		***Pressure dropped to 0 bar***				
0 bar	Water take litre		151	142	144	147	146
4th period	Time, min	**0**	**1**	**2**	**3**	**4**	Average flow
Gauge Pressure:	Flowmeter	23153	23167.6	23182.1	23196.6	23211.2	q litres/min
	Dipmeter		***Pressure dropped to 0 bar***				
0 bar	Water take litre		146	145	145	146	145.5

Remarks:

Water intake fluctuating from 162.75 litres/min to 145.5 litres/min as pressure decreases and dropped to 0 bar during the 1st. Cycle testing after 1 minute testing.
Couldn't built to desired pressure of test, but continue monitoring as accordingly to the time required for the rest of the 2rd cycle to the end cycle of test.

Formation failed after testing with 1.25 bar and lasted for 1 minute only and pressure drop to zero.
Leakage can be seen along the fault plane on hill slope about 1.5m away from the fault plane.

In the bigger picture, the following observations and conclusions are noteworthy:

- We conclude that outcrop studies addressing morphology, clay gouging with different gouging materials and textures can be a very powerful tool to assess faulting processes in the subsurface, and, perhaps to some extent, provide useful input for simulation studies.

- When it comes to rock properties and rock mechanics, it is exactly this where our conclusions differ. The drilled and pressure-tested rocks are undoubtedly weathered. While virgin sandstone appears hard and elastic, the weathered sandstone appears friable, and Ca and Mg cations belonging to cement have been partly removed. Such weathered rocks appear to be utterly different from fresh rock, and the zone of weathering in the Miri area may reach 50m deep. Though fault and gouging properties remain imaged in the weathered rock, the rock composition and strength have changed. There is only one outcrop, formed by a very hard and dense sandstone in the Miri Formation which could offer an idea of fresh rock properties; it was formed after a prominent landslide in 2009 (near the location of Figure 14).

- Therefore, the authors recommend caution when weathered rock properties are applied to simulate subsurface rock properties. Rock property studies in areas of tropical weathering may yield invalid results if applied to virgin rocks.

In summary, from a hydrocarbon exploration standpoint, it makes most sense to consider and integrate all available data: field measurements, simulation results and empirical data, embedded with a sound understanding of the local geology such that realistic scenarios can be developed to achieve better predictions of trapped hydrocarbon accumulations.

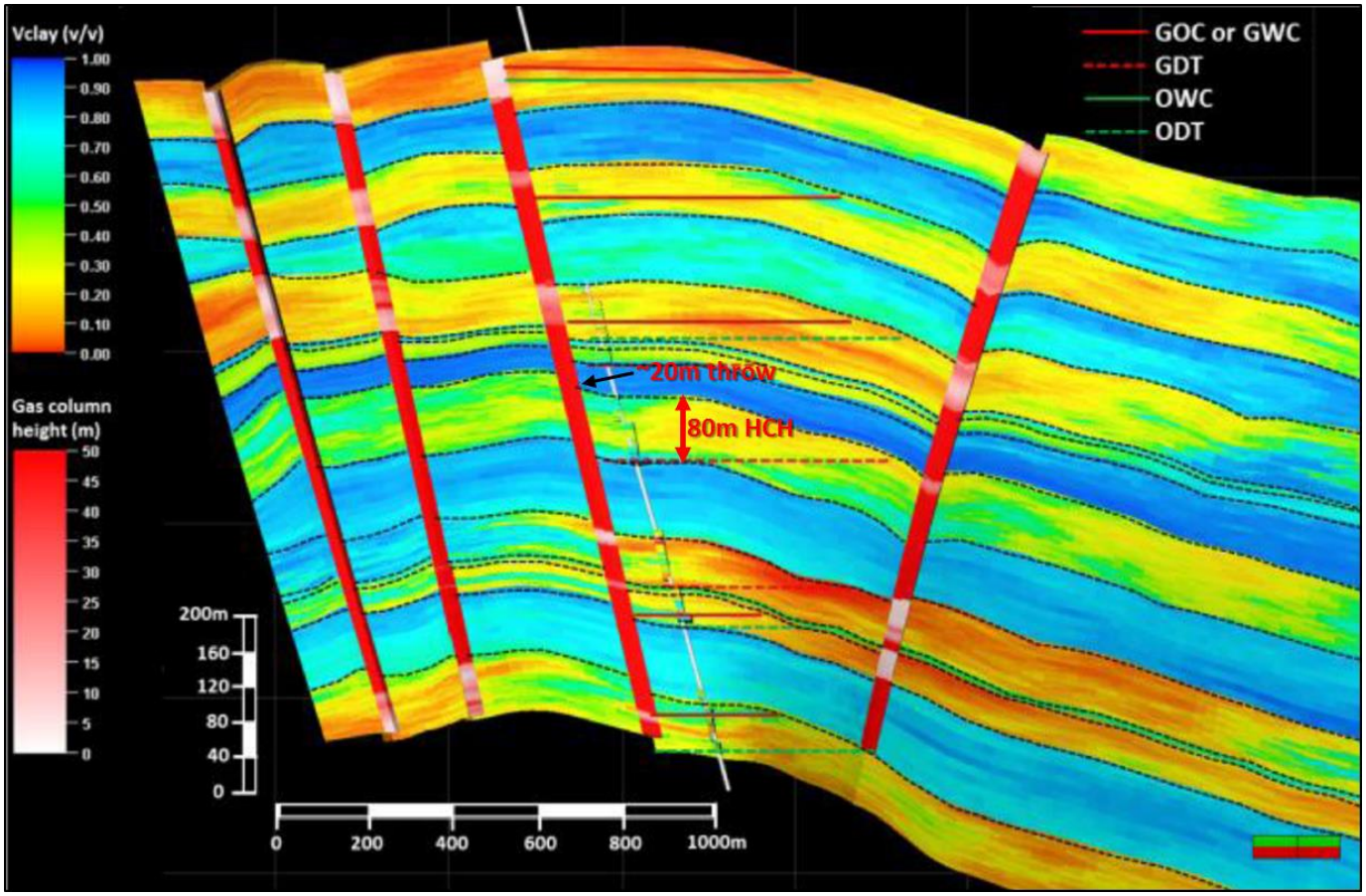


Figure 12: *Cross section showing a Vsh model and faults with potential HCH (hydrocarbon column height, gas case) in comparison with the actual fluid contacts observed by the well (from Uchimura et al., 2014)*

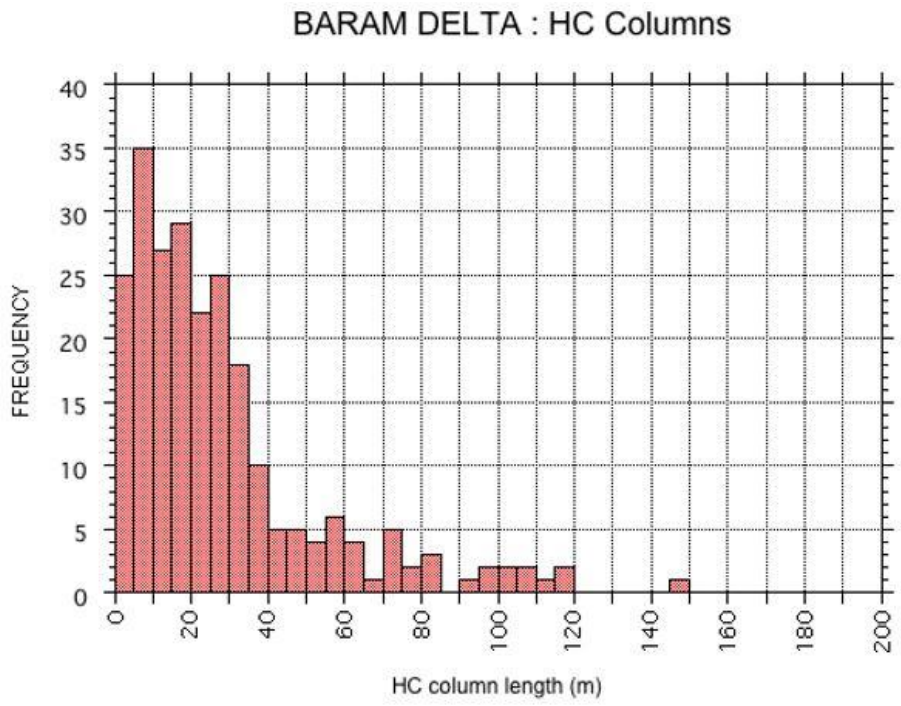


Figure 13: *Hydrocarbon columns from the West Baram Delta fields (from Jong and Shimada, 2009).*



Figure 14: *A field photo of the landslide at a petrol station on Canada Hill, Miri in 2009, where a section of the hill with an elevation of some 50 m collapsed and destroyed houses and the petrol station (credit: Borneo Post online). Another landslide a little distance away exposed the only known unweathered example of Miri Formation sandstone.*

ACKNOWLEDGEMENTS

We thank Mr. Hajime Kusaka, GM Exploration at JX Nippon in Miri (2009-2011) for sponsoring and endorsing field studies. This study has benefited from the discussion with Titus Murray, a fault seal expert with whom we visited the outcrops and conducted a field course together. A student group supervised by A/Professors Dr. Ramasamy Nagarajan and Dr. Prasanna Mohan Viswanathan with the following team members: Aaron Lee Chang Fung, Muhammad Noorasfan Mahmud, William Si Wee Liang and Wilmer Wong Chen Khai contributed significantly to the findings and complimented our earlier work. Our gratitude is also extended to our reviewers for their constructive comments that enhanced the quality of this manuscript.

REFERENCES

Banda, R.M. and Honza, E., 1997. Miocene stratigraphy of northwest Borneo Basin. Bulletin of the Geological Society of Malaysia, 40, p. 1-11.

Bouvier, J.D., Kaars-Sijpesteijn, C.H., Kluesner, D.F., Onyejekwe, C.C. and van der Pal, R.C., 1989. Three-dimensional seismic interpretation and fault sealing investigations, Nun River Field, Nigeria. AAPG Bulletin, 73, p. 1397-1414.

Bretan, P., Yielding, G. and Jones, H., 2003. Using calibrated Shale Gouge Ratio to estimate hydrocarbon column heights. AAPG Bulletin, 87, p. 397–413.

Curtin University Malaysia, 2017. Fault Identification and Their Sealing Capacity in Lambir Formation, Miri, Sarawak, Group Research Thesis submitted for the degree of Bachelor of Science in Applied Geology by: Aaron Lee Chang Fung, Muhammad Noorasfan Mahmud, William Si Wee Liang and Wilmer Wong Chen Khai. Department of Applied Geology (unpublished).

Fristad, T., Groth, A., Yielding, G. and Freeman, B., 1997. Quantitative fault seal prediction: a case study from Oseberg Syd. Norwegian Petroleum Society Special Publication, 7, p. 107–124.

Jev, B.I., Kaars-Sijpesteijn, C.H., Peters, M., Watts, N.L. and Wilkie, J.T., 1993. Akaso field, Nigeria: Use of integrated 3-D seismic, fault slicing, clay smearing, and RFT pressure data on fault trapping and dynamic leakage. AAPG Bulletin, 77, p. 1389– 1404.

Jong. J. and Shimada, M., 2009. Fault Seal Analysis on Adong Kecil Structure and Evaluation Report for FaultRisk™ Fault Seal Analysis Software. Nippon Oil (unpublished).

Jong, J., Kessler, K.L., Noon, S. and Tan, T.Q., 2016. Structural development, depositional Model and petroleum system of Paleogene carbonate of the Engkabang-Karap Anticline, onshore Sarawak. Berita Sedimentologi, 34, p. 5-25.

Kessler, F.L., 2010. The Baram Line in Sarawak: comments on its anatomy, history and implications for potential nonconventional gas deposits. Warta Geologi, 35(3), p. 105-110.

Kessler, F.L and Jong, J., 2010. How to make a map from an outcrop? Houston Geological Society Bulletin, Technical Note, p. 55-59.

Kessler, F.L and Jong, J., 2014. Habitat and C-14 age dating of lignitic terrace sands - implications for uplift on the Borneo coastline during the Holocene. Bulletin of the Geological Society of Malaysia, 60, p. 27-34.

Kessler, F.L. and Jong, J., 2015. Northwest Sarawak: a complete geologic profile from the Lower Miocene to the Pliocene covering the Upper Setap Shale, Lambir and Tukau Formations. Warta Geologi, 41(3-4), p. 45-51.

Kessler, F.L. and Jong, J., 2016. Shape Parameters of clay and quartz clasts in the Neogene Tukau and Lambir Formations, NW Sarawak. Warta Geologi, 42(3-4), p. 63-68.

Kessler, F.L. and Jong, J., 2017a. The roles and implications of several prominent unconformities in Neogene sediments of the greater Miri area, NW Sarawak. Warta Geologi, 43(4), p. 1-8.

Kessler, F.L. and Jong, J., 2017b. Examples of fault architecture and clay gouging in Neogene clastics of the Miri area, Sarawak. Warta Geologi, 43(1), p. 15-20.

Kessler, F.L., Murray, T. and Jong, J., 2010. Faulting and clay gouging in Neogene clastics of the Lambir Formation, Sarawak, Petroleum Geology Conference and Exhibition, KL Convention Centre, PGCE2010 Program Book, p. 313-314.

Lindsay, N.G., Murphy, F.C., Walsh, J.J. and Watterson, J., 1992. Outcrop studies of shale smears on fault surface, in: The

Geological Modelling of Hydrocarbon Reservoirs and Outcrop Analogues. Blackwell Publishing Ltd., p. 113–123.

Oyedele, K.F. and Adeyemi, A.S., 2009. Assessment of fault-zone materials and their impact on hydrocarbon accumulation using integrated Exploration techniques. Journal of American Science, 5, 113–122.

Sandal, T. (ed.), 1996. The geology and hydrocarbon resources of Negara Brunei Darussalam, Brunei Shell Petroleum Co. Sdn. Bhd. and Brunei Museum, 243 p.

Uchimura, R., Yoshikawa, K., Syafiza Adian, Terabe, K., Yasukochi, T., Chin, P.T. and Yii, J., 2014. Verification of the hydrocarbon accumulation in the fault leaned closure with small fault throw: Case study for the Late Miocene Deltaic Sandstone Reservoirs (Sarawak Cycle V) Block D, Sarawak, Malaysia. International Petroleum Technology Conference, KLCC, Kuala Lumpur, DOI: 10.2523/IPTC-18174-MS.

van der Zee, W., Urai, J.L. and Pascal, D.R., 2003. Lateral clay injection into normal faults. GeoArabia, 8(3), p. 501-522.

van der Zee, W. and Urai, J.L., 2005. Processes of normal fault evolution in a siliciclastic sequence: a case study from Miri, Sarawak, Malaysia. Journal of Structural Geology, 27, p. 2281–2300.

Vrolijk, P.J., Urai, J.L. and Kettermann, M., 2016. Clay smear: Review of mechanisms and applications. Journal of Structural Geology, 86, p. 95–152.

Yielding, G., 2002. Shale gouge ratio - Calibration by geohistory. Norwegian Petroleum Society Special Publication, 11, p. 1–15.

Yielding, G., Freeman, B. and Needham, T., 1997. Quantitative fault seal prediction: AAPG Bulletin, 81, p. 897-917.